HHS Public Access

Author manuscript

Cytometry B Clin Cytom. Author manuscript; available in PMC 2017 November 01.

Published in final edited form as:

Cytometry B Clin Cytom. 2016 November ; 90(6): 499–505. doi:10.1002/cyto.b.21223.

Relationship of Light Scatter Change and Cdc42-Regulated Actin Status

Lin Hong[1,2], **Stephanie Chavez**[1], **Yelena Smagley**[1], **Alexandre Chigaev**[1], and **Larry A. Sklar**[1,2,3,*]

[1]Department of Pathology, University of New Mexico, Albuquerque, New Mexico 87131

[2]UNM Center for Molecular Discovery, University of New Mexico, Albuquerque, New Mexico 87131

[3]Cancer Research and Treatment Center, University of New Mexico, Albuquerque, New Mexico 87131

Abstract

Background—Cdc42 GTPase has important roles in regulating intracellular actin reorganization. The current methods to monitor actin changes are typically complex and point by point.

Methods—The effects of Cdc42 inhibitors on the side scatter changes were tested in a newly developed continuous assay using the flow cytometer. Staining with fluorescently labeled phalloidin was used for comparison.

Results—Cdc42 specific inhibitors caused dose-dependent changes of both the right angle side scatter and the phalloidin stained-actin.

Conclusions—The right angle light scatter change can be used as a method to circumvent phalloidin staining and be an early convenient step in screening Cdc42 inhibitors.

Keywords

Cdc42; actin; polymerization; side scatter; phalloidin

Introduction

Rho family GTPases are low molecular weight guanine nucleotide binding proteins. Rho GTPases switch between the active GTP- and the inactive GDP- binding states. A representative and well-studied member of the Rho family GTPases is Cdc42. Early work found that when the protein was inactivated by toxin B, a monoglucosyltransferase from *Clostridium difficile*, actin stress fibers in host cells could not form normally (1,2). Later, the function of Cdc42 was further elucidated as essential for the formation of filopodia, which are the microspikes made of actin polymers at the leading edge of cells moving along a chemotactic gradient (3). Cdc42 has since then been established as an essential regulator of

*Correspondence: Dr. Larry A. Sklar, MSC 084640, 1 University of New Mexico, Albuquerque, NM 87131, USA, lsklar@salud.unm.edu.

cytoskeleton transformation which requires dynamic actin polymerization and depolymerization (4,5). Malfunction of the Rho family GTPases including Cdc42, has been associated with various diseases, such as cancer cell metastasis and pathogen invasions (6,7). The motility of leukocytes and cancer cells as well as the internalization of the pathogenic bacteria depend on properly regulated actin polymerization and depolymerization (8,9). During actin polymerization, G-actin monomers are linked together to form F-actin polymers. Previously, one way to measure actin polymerization was to use a DnaseI assay to determine the disappearance of the G-actin monomers (10). Later, phalloidin was found to be able to bind to F-actin and stabilize it. Staining with fluorescently labeled phalloidin has since then been used as a standard to quantify actin polymers (11). Nowadays, there are also in vitro assays to label actin in the cell lysate (12), and biomimetic assays where small beads are covered with protein complexes that are involved in actin polymerization (13). These assays have improved our understanding of the process of actin reorganization and the required cellular components. However, they also have inherent limitations. Either samples were taken from separate time points, or actin polymer did not form in a physiologically relevant environment. Yuli *et al.* and Sklar *et al.* had reported a right angle light scatter assay associated with actin polymer formation and degradation in real-time using a fluorometer (14-17). However, the relation between the light scatter changes and the actin reorganization was later questioned in two reports (18,19). In these reports, either the light scatter was evaluated in an intermittent and time-resolved manner, or the experiments included stimulant agonists at micro- to millimolar levels which can lead to other changes such as cell aggregation. Here, we demonstrated that Cdc42 specific inhibitors caused dose-dependent changes of the right angle side scatter that was measured in a continuous flow cytometer-based assay where low nanomolar peptide agonists were used. Since Cdc42 has established roles in actin polymerization and depolymerization, the present results suggest an association between the Cdc42-dependent side scatter changes and the actin status.

Materials and Methods

N-Formyl-Met-Leu-Phe-Phe (fMLFF) was purchased from Sigma-Aldrich. NBD-phalloidin was from Life Technologies. 37% formaldehyde and lysophosphatidyl choline were from Sigma-Aldrich. Mono-Poly Resolving Medium was from MP Biomedicals. FACScan™ was from BD Biosciences.

Polymorphonuclear Leucocytes Preparation

Polymorphonuclear Leucocytes (PMNs) were separated from human blood drawn from healthy volunteers using Mono-Poly Resolving Medium (M-PRM) according to the protocols provided by the manufacturers. Briefly, in a sterile test tube was placed 3 mL of M-PRM followed by a layer of 3.5 mL of human venous blood drawn within 6 h. Centrifugation at 300 xg at room temperature for 30 min divided the blood into separate layers containing mononuclear leucocytes, PMNs, red blood cells, and plasma. The PMNs were withdrawn with a clear Pasteur pipette, suspended in RPMI medium and kept on ice. One hundred fold dilution of the cell suspension was used to measure cell concentration with the trypan blue staining method. PMNs from four healthy donors were collected. For formyl peptide titration and assay development, PMNs from two donors were used and

repetition numbers are 2 and 3, respectively. For other experiments, PMNs from four donors were used and repetition numbers are 2, 3, 3 and 3, respectively.

Right Angle Side Scatter Kinetics Assay

PMNs were diluted to 1×10^6 cells/mL using RPMI medium supplemented with 1 mM $CaCl_2$. All the experiments were performed at 37 °C. A tube containing 1 mL of PMNs at 1×10^6 cells/mL was mounted to the FACScan™ flow cytometer and right angle side scatter was monitored continuously with excitation and emission at 488 nm. The cells were constantly stirred at 80 rpm. A custom made external unit connected to a Lauda water bath was used to maintain the temperature while stirring was provided by the Multi Stirrer MC303 from Scinics. The flow rate was set as 12 μL/min. Compound or DMSO and *N*-formyl peptide were added at different times. To optimize the assay conditions, the concentration of the peptide, the addition order and the interval time between additions were varied.

F-Actin Staining

F-actin staining using NBD-phalloidin was carried out as described previously with minor modifications (14,15). PMNs were from the same preparation as in the light scatter kinetic assays and all the experiments were carried out at 37 °C. PMNs were first equilibrated at the desired temperature. At 1 min, either compound or DMSO was added to cells suspended at 1×10^6 cells/mL. At 2 min, *N*-formyl peptide at 0.1 nM was added. Throughout the process, aliquots of the cell suspension were taken at different times and added to an equal volume of 7.4% formaldehyde. The samples were incubated overnight at 4 °C. On the day of analysis, the fixed samples were permeabilized and stained with an equal volume of a mixture of 7.4% formaldehyde, 0.2 mg/mL lysophosphatidyl choline, and 330 nM NBD-phalloidin. The mixtures were incubated at room temperature for 1 h before being analyzed on the FACScan™ flow cytometer. The excitation and emission wavelength was 488 nm and 530/30 nm, respectively. Five thousand events were collected.

Results

Dose-dependent Effects of N-formyl Peptide on Right Angle Side Scatter

The main population of the isolated PMNs was gated on the forward scatter and side scatter plot. The median of the right angle side scatter was found to change in a dose-dependent manner upon addition of *N*-formyl peptide (Figure 1). The changes had two phases. In the first phase, immediately after agonist stimulation, the right angle side scatter decreased sharply within seconds; while in the second phase, the side scatter recovered and stabilized at extended time. The extent of the decrease and the rate of the recovery depended on the concentration of the agonist used. The changes were most obvious when the reading of the right angle side scatter was normalized to the average value obtained prior to agonist stimulation. For subsequent right angle side scatter assay development, the formyl peptide at 0.1 nM was chosen (Figure 1G). At this concentration, the changes in the side scatter had an optimal signal to noise ratio, while the amount of the peptide agonists was not high enough to saturate the peptide receptors on the cell surface (20) and impair the observation of changes caused by Cdc42 inhibitor intervention.

Cdc42 dependence of Right Angle Side Scatter

To explore whether the observed changes of the right angle side scatter were associated with the intracellular actin status, inhibitors of Cdc42, a GTPase with established roles in regulating actin polymerization changes, were used. In developing the assay, the order of the reagent addition was examined (Figure 2A and B). It was found that the changes of the right angle side scatter were more apparent if cells were first treated with a Cdc42 inhibitor followed by agonist stimulation than otherwise. When the agonist peptide was added before the Cdc42 inhibitor, the difference between the inhibitor and DMSO treatment was less obvious. This was possibly due to the slow kinetics for the inhibitor to enter the cells and reach its target (21). By the time the compound was inside the cell, noticeable changes from the right angle side scatter, that may reflect the dynamic actin polymerization and depolymerization and only last for seconds, had been missed. It was also observed that compound addition caused a transient increase of the right angle side scatter (Figure 2A, green). This should not interfere with the later changes caused by *N*-formyl peptide since the right angle side scatter had returned to the baseline by the time of the peptide addition (Figure 2C). This was further confirmed by the fact that if the formyl peptide was added five minutes instead of one minute later to allow enough time for the perturbed right angle side scatter to return to the norm, the observed changes after the peptide stimulation were comparable to that with the one-minute addition interval (Figure 2D). The one-minute interval was chosen to expedite the assay to have a fast turnaround.

F-actin Staining Using NBD-phalloidin

It has been established that phalloidin selectively binds F-actin polymers while sparing G-actin monomers. Fluorescent phalloidin staining of F-actin has been a standard method to monitor actin status changes in cells. The final readout can be either through flow cytometer or microscopy (12). This method was used here to measure actin reorganization caused by the Cdc42 inhibitor. The results showed that when cells were stimulated with the *N*-formyl peptide, there was a nearly instantaneous increase of the fluorescent phalloidin stained F-actin polymer followed by a decline at a slower rate (Figure 3A and B). The changes concurred with the initial decrease and the subsequent recovery observed in the right angle side scatter assay (Figure 3C and D). When the PMNs were pretreated with the Cdc42 inhibitors, the extent of the peptide-induced actin polymerization changes was reduced. This occurred with both of the Cdc42 inhibitors tested. CID2950007 was shown to delay the actin polymerization and depolymerization in a dose dependent manner (Figure 3E and 3F), while CID44216842 more obviously facilitated the depolymerization process (Figure 3B). The different solubility and permeability of the two Cdc42 inhibitors possibly contributed to the observed difference. CID44214842 has increased solubility and permeability compared with CID2950007 (21), and thus can possibly get into cell and bind to its target more rapidly. By the time of the peptide addition, the effects of CID44216842 could already be observed and more obviously on the depolymerization phase, while CID2950007 bound to its target more slowly and its effects were manifested as delaying the actin polymerization.

Using Cdc42 Inhibitors to Test Effects on Side Scatter

With the assay conditions optimized (Figure 2) and correlation with phalloidin staining demonstrated (Figure 3), Cdc42-specific inhibitors, CID2950007 and CID44216842 (21,22), were used to test their effects on side scatter changes stimulated by *N*-formyl peptide. It was found that the amplitude of the side scatter decrease induced by *N*-formyl peptide was mitigated in a dose-dependent manner by the CID2950007 treatment at each of the three peptide concentrations used (Figure 4A-C). CID44216842 has comparable mitigating effects as CID2950007 at 10 μM (Figure 3D). Since these compounds are Cdc42-specific inhibitors (21) and Cdc42 has established roles in actin reorganization, the observed Cdc42-dependent effects were consistent with an association between the right angle scatter and the actin status under these experimental conditions.

Discussion

The study described here, where the PMNs were stimulated with *N*-formyl peptide, presented a cellular model of the immune responses that occur when pathogens are encountered. The *N*-formyl peptide simulates toxins released from pathogens. The role of Cdc42 in actin polymerization was initially revealed by studying pathogen invasion (23). It was noted that pathogenic bacteria can release toxins that activate the GTPase. Some bacteria can induce a quick actin polymerization followed by depolymerization (24-26). It is understandable that when a pathogen encounters host cells, the initial actin polymerization will contribute to pathogen internalization whereas sustaining actin polymerization will inhibit the motility of the host cells, and hamper the spreading of the pathogen (23). Therefore subsequent actin depolymerization is necessary. Cdc42 promotes actin polymerization through several pathways. By interacting with the Wiskott-Aldrich syndrome protein (WASP) and WASP-family verprolin-homologous protein (WAVE), Cdc42 releases their auto inhibition which then activate the actin-related protein-2/3 (ARP2/3) complex (27-31). The Arp2/3 complex directly instructs actin monomers to be added to the leading barbed ends of actin polymers (32). Moreover, activated Cdc42 can interact and activate the downstream effector protein p21-activating kinases (PAK). PAK stimulates LIM domain kinase (LIMK) which inhibits the depolymerization protein cofilin (33). On the other hand, the depolymerization process has been associated with either Cdc42 inactivation or secretion (34). Accumulating evidence has suggested that activated Cdc42 is degraded through the ubiquitination pathway. The degraded Cdc42 releases inhibition of cofilin which then break the actin polymer at the minus end (35,36).

In both the right angle side scatter and the actin staining experiments, if the PMNs were pretreated with Cdc42 inhibitors, the side scatter and the stained actin changed in a dose-dependent manner. From the actin staining experiment, either polymerization was delayed as in the case of CID2950007, or the depolymerization process was expedited as for CID44216842. Difference in solubility and permeability of the compounds used may play a role. It should be noted that previous studies have shown that neither the Cdc42 inhibitors nor the formyl peptide causes any cytotoxicity at the concentrations used. Therefore, the observe effects are not related to cell killing (17,20,21).

Importantly, we demonstrated that *N*-formyl peptide can cause correlated changes of the right angle side scatter and the phalloidin-stained actin responses (Figure 3A and C, and Figure 3B and D) although distinct kinetic resolution was not apparent. Moreover, Cdc42 inhibitors showed mitigating effects on both changes. Since Cdc42 has established roles in actin reorganization, the correlated changes from the two readouts are consistent with an association of the right angle light scatter and the actin status. Compared with the phalloidin staining and other time-resolved assays, the right angle side scatter assay allowed continuous measurement of actin changes in intact cells in real-time. The initial responses of the stimulated cells can be captured within seconds. Also, the instrument settings used in the present right angle side scatter assay are easily accessible. The excitation wavelength 488 nm is commonly installed on almost all the laboratory flow cytometers. Previously, fluorometers with excitation wavelength at 360 nm were used to measure the right angle light scatter (15). However, the fluorometer measurement required bulk volume readings susceptible to interference from other activities in the medium whereas the flow cytometer analyzes single particles with increased sensitivity. Overall, the data presented here showed the actin reorganization caused by Cdc42 and the corresponding side scatter changes. To address the previous doubt of using the side scatter to account for the actin status, the present results confirmed the correlation between the two events when measured continuously. Moreover, the light scatter assay developed here is a real-time and phenotypic assay that can be used to identify other Cdc42 inhibitors which interfere with actin polymer reorganization.

Acknowledgments

The raw data obtained from the FACScan™ flow cytometer was analyzed by the HyperView® software developed by Dr. Bruce Edward at the University of New Mexico. The authors thank Anna Waller for helpful discussions, and Matthew Garcia and Mark Carter for technical assistance.

This work was supported by UNMCMD MLPCN NIH grant U54MH084690 and R01HL081062 to Larry A. Sklar.

References

1. Prepens U, Just I, von Eichel-Streiber C, Aktories K. Inhibition of Fc epsilon-RI-mediated activation of rat basophilic leukemia cells by Clostridium difficile toxin B (monoglucosyltransferase). J Biol Chem. 1996; 271:7324–9. [PubMed: 8631752]
2. Aktories K. Bacterial protein toxins that modify host regulatory GTPases. Nat Rev Microbiol. 2011; 9:487–98. [PubMed: 21677684]
3. Nobes CD, Hall A. Rho, rac, and cdc42 GTPases regulate the assembly of multimolecular focal complexes associated with actin stress fibers, lamellipodia, and filopodia. Cell. 1995; 81:53–62. [PubMed: 7536630]
4. Ridley AJ. Rho GTPases and cell migration. J Cell Sci. 2001; 114:2713–22. [PubMed: 11683406]
5. Tapon N, Hall A. Rho, Rac and Cdc42 GTPases regulate the organization of the actin cytoskeleton. Curr Opin Cell Biol. 1997; 9:86–92. [PubMed: 9013670]
6. Antoine-Bertrand J, Villemure JF, Lamarche-Vane N. Implication of rho GTPases in neurodegenerative diseases. Curr Drug Targets. 2011; 12:1202–15. [PubMed: 21561415]
7. Rathinam R, Berrier A, Alahari SK. Role of Rho GTPases and their regulators in cancer progression. Front Biosci. 2012; 17:2561–71.
8. Parsons JT, Horwitz AR, Schwartz MA. Cell adhesion: integrating cytoskeletal dynamics and cellular tension. Nat Rev Mol Cell Biol. 2010; 11:633–43. [PubMed: 20729930]

9. Hynes RO. The extracellular matrix: not just pretty fibrils. Science. 2009; 326:1216–9. [PubMed: 19965464]
10. Snabes MC, Boyd AE 3rd, Pardue RL, Bryan J. A DNase I binding/immunoprecipitation assay for actin. J Biol Chem. 1981; 256:6291–5. [PubMed: 6263912]
11. Howard TH, Meyer WH. Chemotactic peptide modulation of actin assembly and locomotion in neutrophils. J Cell Biol. 1984; 98:1265–71. [PubMed: 6232281]
12. Mitchell T, Lo A, Logan MR, Lacy P, Eitzen G. Primary granule exocytosis in human neutrophils is regulated by Rac-dependent actin remodeling. Am J Physiol Cell Physiol. 2008; 295:C1354–65. [PubMed: 18799653]
13. Wiesner S, Helfer E, Didry D, Ducouret G, Lafuma F, Carlier MF, Pantaloni D. A biomimetic motility assay provides insight into the mechanism of actin-based motility. J Cell Biol. 2003; 160:387–98. [PubMed: 12551957]
14. Eberle M, Traynor-Kaplan AE, Sklar LA, Norgauer J. Is there a relationship between phosphatidylinositol trisphosphate and F-actin polymerization in human neutrophils? J Biol Chem. 1990; 265:16725–8. [PubMed: 2211588]
15. Omann GM, Porasik MM, Sklar LA. Oscillating actin polymerization/depolymerization responses in human polymorphonuclear leukocytes. J Biol Chem. 1989; 264:16355–8. [PubMed: 2550438]
16. Yuli I, Snyderman R. Rapid changes in light scattering from human polymorphonuclear leukocytes exposed to chemoattractants. Discrete responses correlated with chemotactic and secretory functions. J Clin Invest. 1984; 73:1408–17. [PubMed: 6715544]
17. Sklar LA, Omann GM, Painter RG. Relationship of actin polymerization and depolymerization to light scattering in human neutrophils: dependence on receptor occupancy and intracellular Ca++. J Cell Biol. 1985; 101:1161–6. [PubMed: 4040917]
18. Keller HU, Fedier A, Rohner R. Relationship between light scattering in flow cytometry and changes in shape, volume, and actin polymerization in human polymorphonuclear leukocytes. J Leukoc Biol. 1995; 58:519–25. [PubMed: 7595052]
19. Kraus E, Niederman R. Changes in neutrophil right-angle light scatter can occur independently of alterations in cytoskeletal actin. Cytometry. 1990; 11:272–82. [PubMed: 2318082]
20. Chigaev A, Buranda T, Dwyer DC, Prossnitz ER, Sklar LA. FRET detection of cellular alpha4-integrin conformational activation. Biophys J. 2003; 85:3951–62. [PubMed: 14645084]
21. Hong L, Kenney SR, Phillips GK, Simpson D, Schroeder CE, Noth J, Romero E, Swanson S, Waller A, Strouse JJ. Characterization of a Cdc42 protein inhibitor and its use as a molecular probe. J Biol Chem. 2013; 288:8531–43. others. [PubMed: 23382385]
22. Surviladze, Z.; Waller, A.; Strouse, JJ.; Bologa, C.; Ursu, O.; Salas, V.; Parkinson, JF.; Phillips, GK.; Romero, E.; Wandinger-Ness, A. Probe Reports from the NIH Molecular Libraries Program. Bethesda (MD): 2010. A Potent and Selective Inhibitor of Cdc42 GTPase.. others
23. Boquet P, Lemichez E. Bacterial virulence factors targeting Rho GTPases: parasitism or symbiosis? Trends Cell Biol. 2003; 13:238–46. [PubMed: 12742167]
24. Lemichez E, Lecuit M, Nassif X, Bourdoulous S. Breaking the wall: targeting of the endothelium by pathogenic bacteria. Nat Rev Microbiol. 2010; 8:93–104. [PubMed: 20040916]
25. Aktories K, Barbieri JT. Bacterial cytotoxins: targeting eukaryotic switches. Nat Rev Microbiol. 2005; 3:397–410. [PubMed: 15821726]
26. Yarmola EG, Bubb MR. How depolymerization can promote polymerization: the case of actin and profilin. Bioessays. 2009; 31:1150–60. [PubMed: 19795407]
27. Pantaloni D, Le Clainche C, Carlier MF. Mechanism of actin-based motility. Science. 2001; 292:1502–6. [PubMed: 11379633]
28. Kim AS, Kakalis LT, Abdul-Manan N, Liu GA, Rosen MK. Autoinhibition and activation mechanisms of the Wiskott-Aldrich syndrome protein. Nature. 2000; 404:151–8. [PubMed: 10724160]
29. Miki H, Sasaki T, Takai Y, Takenawa T. Induction of filopodium formation by a WASP-related actin-depolymerizing protein N-WASP. Nature. 1998; 391:93–6. [PubMed: 9422512]
30. Prehoda KE, Scott JA, Mullins RD, Lim WA. Integration of multiple signals through cooperative regulation of the N-WASP-Arp2/3 complex. Science. 2000; 290:801–6. [PubMed: 11052943]

31. Gruenheid S, Finlay BB. Microbial pathogenesis and cytoskeletal function. Nature. 2003; 422:775–81. [PubMed: 12700772]
32. Carlier MF, Le Clainche C, Wiesner S, Pantaloni D. Actin-based motility: from molecules to movement. Bioessays. 2003; 25:336–45. [PubMed: 12655641]
33. Bamburg JR. Proteins of the ADF/cofilin family: essential regulators of actin dynamics. Annu Rev Cell Dev Biol. 1999; 15:185–230. [PubMed: 10611961]
34. Aktories K, Schwan C, Papatheodorou P, Lang AE. Bidirectional attack on the actin cytoskeleton. Bacterial protein toxins causing polymerization or depolymerization of actin. Toxicon. 2012; 60:572–81. [PubMed: 22543189]
35. Wang W, Eddy R, Condeelis J. The cofilin pathway in breast cancer invasion and metastasis. Nat Rev Cancer. 2007; 7:429–40. [PubMed: 17522712]
36. Ridley AJ. Rho GTPases and actin dynamics in membrane protrusions and vesicle trafficking. Trends Cell Biol. 2006; 16:522–9. [PubMed: 16949823]

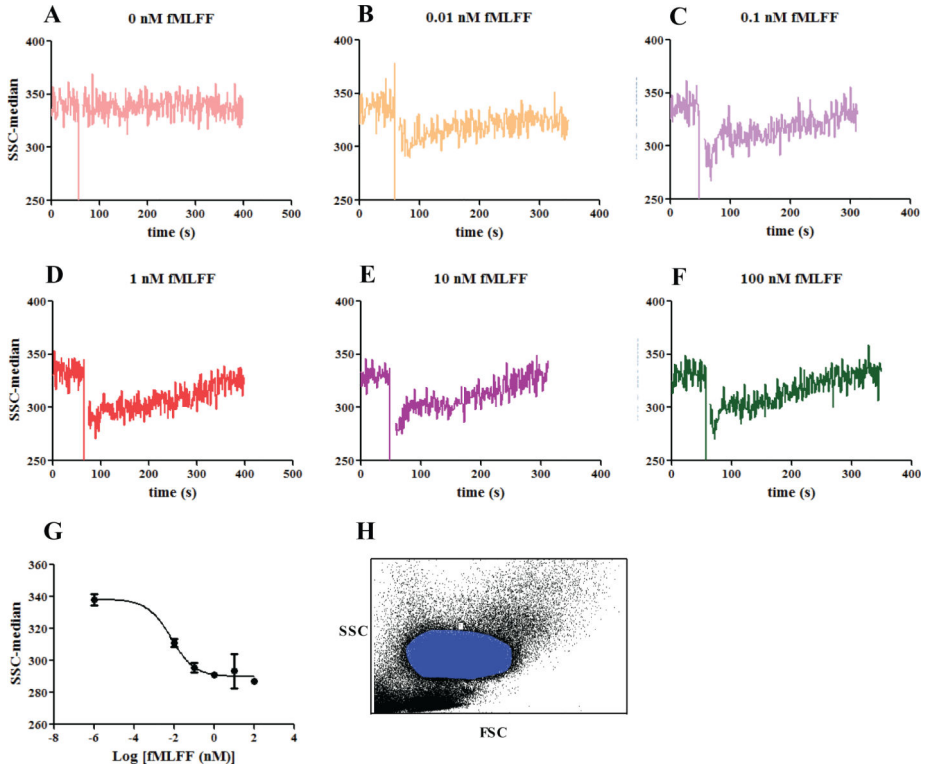

Figure 1.

Right angle side scatter reading of PMNs stimulated with different concentrations of *N*-formyl peptide. (A) DMSO control; (B) 0.01 nM fMLFF; (C) 0.1 nM fMLFF; (D) 1 nM fMLFF; (E) 10 nM fMLFF; (F) 100 nM fMLFF. (G) The side scatter changes caused by fMLFF were fitted to the dose-response equation with variable slope using GraphPad Prism 5. EC50= 0.007 nM. Ten data points right after fMLFF peptide stimulation were averaged and used for the graph. (H) A representative FSC versus SSC plot of the blood samples and the gating of PMNs (blue area) are shown. The PMNs were withdrawn from two healthy donors. For donor 1, the experiment was conducted in duplicates; for donor 2, the experiment was done in triplicate. Representative curves are shown.

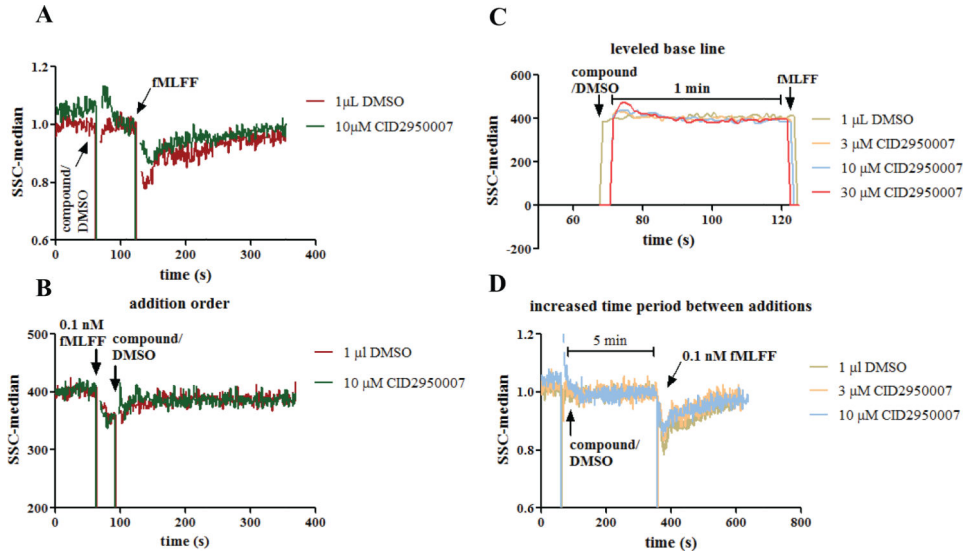

Figure 2.

Right angle side scatter assay development. (A) Compound or DMSO was added to PMN cells. When the right angle side scatter baseline was stabilized one minute later, 0.1 nM fMLFF was added. The compound showed different effects from DMSO. (B) fMLFF was added before compound or DMSO. No apparent difference was observed between compound and DMSO. (C) Expanded view of the right angle side scatter reading between compound/DMSO and fMLFF additions. The baseline reading had stabilized before fMLFF addition. (D) fMLFF was added 5 min after the compound or DMSO. The dose-dependent effects of CID2950007 are comparable to that when fMLFF was added 1 min later. Experiments were conducted using PMNs from two healthy donors and repetition numbers are 2 and 3, respectively. Representative curves are shown. For (A) and (D), the right angle side scatter reading was normalized by being divided with an average of the readings before the fMLFF addition. Ten time points were averaged.

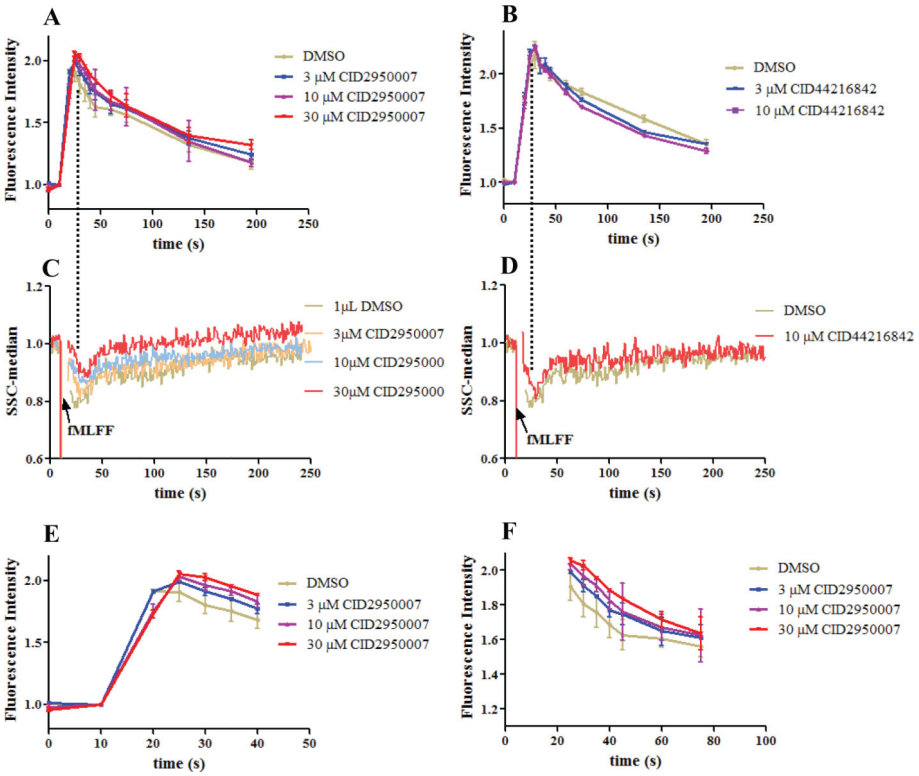

Figure 3.

Fluorescent phalloidin staining assay for comparison. (A) Fluorescence readings of PMNs treated with CID2950007 or DMSO followed by fMLFF. (B) As in (A) except the compound is CID44216842 which facilitated depolymerization. (C) Right angle side scatter readings of PMNs as treated in (A). The changes of readings were coincident with that in (A) without distinct resolution. (D) Right angle side scatter readings of PMNs as treated in (B). The changes of readings were coincident with that in (B) without distinct resolution. (E) Expanded view of (A) for the first 40 s. CID2950007 dose dependently delayed the polymerization process. The slope of the red line was smaller than that of the purple, blue and grey lines in order. (F) Expanded view of (A) after the first 25 s. The depolymerization process was also dose dependently delayed. Both the fluorescence and the side scatter readings were normalized by being divided with an average of the readings before the fMLFF addition. For experiments shown in Figure 3B and D, PMNs from two healthy donors were used and repetition numbers are 2 and 3, respectively, while for other experiments, PMNs from four healthy donors were used and repetition numbers are 2, 3, 3 and 3, respectively.

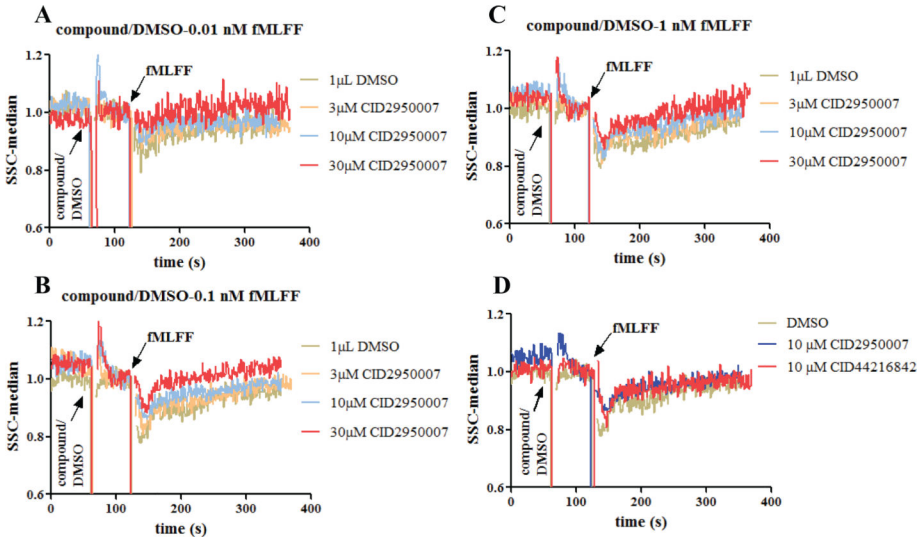

Figure 4.

The effects of the Cdc42 inhibitors on the right angle side scatter when the PMNs were stimulated with different concentrations of fMLFF. (A) CID2950007 and 0.01 nM fMLFF; (B) CID2950007 and 0.1 nM fMLFF; (C) CID2950007 and 1 nM fMLFF; (D) both CID2950007 and CID44216842 and 0.1 nM fMLFF. The right angle side scatter reading was normalized as described in Figure 2. For experiments shown in Figure 4B, PMNs from four healthy donors were used and repetition numbers are 2, 3, 3 and 3, respectively, while for other experiments, PMNs from two healthy donors were used, and repetition numbers are 2 and 3, respectively.